

Michael G. Kucherenko , Tatiana M. Chmereva 

Center of Laser and Informational Biophysics, Orenburg State University, Orenburg, Russia

(*Corresponding author's e-mail: elibph@yandex.ru)

Quantum Kinetics of the Electronic Energy Transformation in Molecular Nanostructures

A quantum theory of electronic energy transfer in a layered nanostructure with molecular J-aggregates of polymethine dyes was proposed. An expression for the exciton-plasmon bond energy depending on various parameters of the system was given. The rate of non-radiative Förster resonance energy transfer (FRET) from surface plasmon polaritons (SPPs) of a metal substrate to Frenkel excitons of J-aggregates was determined and dispersion dependences for hybrid states were obtained. It was established that the energy transfer rate can reach values of 10^{12} – 10^{13} s⁻¹, and the value of the Rabi splitting is up to 100 MeV. The kinetics of the process under strong exciton-plasmon interaction was investigated. The time dependence of the energy exchange between the system components had the form of damped oscillations depending on the relaxation parameters, the Rabi frequency, and the response to resonance. In addition, the exciton FRET between two parallel monolayers of J-aggregates of polymethine dyes separated by a nanometer-thick metal film was investigated. It was found that the presence of the metal layer increases the FRET rate. The spin evolution of a pair of two triplet (T) molecules localized in the nano-cell region under the over-barrier jumps regime in a magnetic field was studied. The influence of the parameters of the two-dimensional potential on the frequency of inter-dimensional motions and the population of triplets was considered. The spin dynamics of molecular T-T pairs in the magnetic field of a ferromagnetic globular nanoparticle under free surface diffusion of a spin-carrying molecule was investigated.

Keywords: non-radiative energy transfer, surface plasmon, J-aggregate, Frenkel exciton, triplet-triplet annihilation, dispersion curves, spin dynamics, globular nanoparticle, Rabi splitting.

Contents

1. Plasmon-exciton dynamics and relaxation in a planar system with a monolayer of J-aggregates of polymethine dyes
 - 1.1 Transfer of exciton excitation energy between two monolayers of J-aggregates
 - 1.2 Energy transfer in a cylindrical nanostructure consisting of a metal core and a coaxial shell with phosphor molecules
2. Magnetic field modulation of the rate of triplet-triplet annihilation of electronic excitations in nanostructures
- Conclusions

1. Plasmon-exciton dynamics and relaxation in a planar system with a monolayer of J-aggregates of polymethine dyes

A number of papers [1–3] consider the strong coupling of exciton and plasmon states in nanostructures with J-aggregates, which leads to the formation of hybrid quasiparticles. In [3], the plasmon-exciton interaction was studied in a nanostructure of parallel layers: a metal substrate and two non-conducting layers with different electrical constants. In a dielectric medium, a monolayer of J-aggregates of polymethine dye molecules is located at the interface. Upon photoexcitation of the sandwich structure, Frenkel excitons appear in the quasi-two-dimensional layer of molecular J-aggregates that interact with surface plasmon polaritons (SPPs) of the metal base.

The configuration of the system under study is shown in Figure 1. In the case of weak coupling of exciton and plasmon (EP) states, calculations of the energy transfer rate from the surface plasmon polariton to molecular J-aggregates were carried out within the framework of quantum mechanical perturbation theory. In the case of a strong coupling of excitons and plasmons, the effect of the dielectric medium and the thickness of the layer l on the Rabi splitting (EP interaction energy) at strict resonance was investigated.

The hybrid EP state occurs at the intersection of the dispersion curves in Figure 2, and its energy is [3] as

$$E(\mathbf{k}) = \frac{1}{2} \left(E_{ex}(\mathbf{k}) + \hbar\omega(k) \pm \sqrt{(E_{ex}(\mathbf{k}) - \hbar\omega(k))^2 + 4|V_{10,01}(\mathbf{k})|^2} \right), \quad (1)$$

where $E_{ex}(\mathbf{k})$ is the energy of the 2d exciton, $\hbar\omega(k)$ is the energy of the 2d polariton, $V_{10,01}(\mathbf{k})$ is the matrix element of the EP-coupling, \mathbf{k} is the wave vector of the EP hybrid, $k = |\mathbf{k}|$.

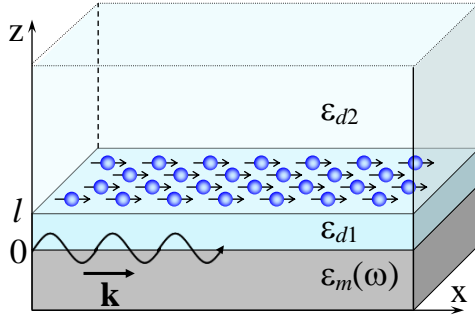


Figure 1. Mutual arrangement of the layers of the hybrid JDM system

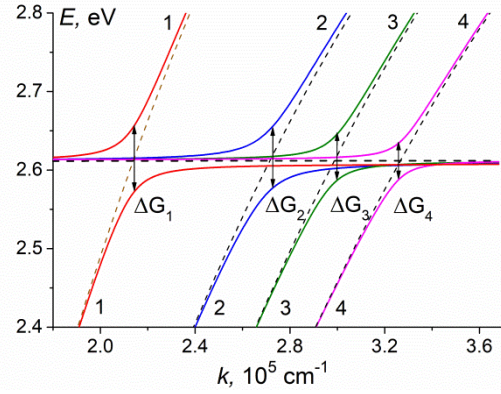


Figure 2. Dispersion curves of hybrid exciton-plasmon quasiparticles for different permittivity values ε_{d2}

It is convenient to represent the EP-interaction in the formalism of secondary quantization. In [4, 5] the quasi-static approximation was used, in which the potential of the SPP field was determined on the basis of the Laplace equation. But already in [3] the intensity of the field created by the SPP was determined from Maxwell's equations. In the approach [6] the time-average field energy of the SPP was quantized by replacing the field strengths with the operators of destruction and generation of SPP with the wave vector \mathbf{k} .

The electric field strength operators of the SPP in metal $z < 0$

$$\hat{\mathbf{E}}_m(\mathbf{r}, z, t) = \sum_{\mathbf{k}} \sqrt{\frac{2\pi\hbar\omega}{SL(k)}} \left(\mathbf{e}_{\mathbf{k}} - i \frac{k}{k_z^m} \mathbf{e}_z \right) e^{k_z^m z} e^{i(\mathbf{k}\mathbf{r} - \omega t)} a_{\mathbf{k}} + H.c. \quad (2)$$

in the dielectric layer $0 \leq z \leq l$

$$\hat{\mathbf{E}}_{d1}(\mathbf{r}, z, t) = \sum_{\mathbf{k}} \sqrt{\frac{2\pi\hbar\omega}{SL(k)}} \left\{ \left(\mathbf{e}_{\mathbf{k}} + i \frac{k}{k_z^{d1}} \frac{f}{d} \mathbf{e}_z \right) \text{ch}(k_z^{d1} z) - \left(\frac{f}{d} \mathbf{e}_{\mathbf{k}} + i \frac{k}{k_z^{d1}} \mathbf{e}_z \right) \text{sh}(k_z^{d1} z) \right\} e^{i(\mathbf{k}\mathbf{r} - \omega t)} a_{\mathbf{k}} + H.c. \quad (3)$$

in a half — space $z > l$, filled with a dielectric

$$\hat{\mathbf{E}}_{d2}(\mathbf{r}, z, t) = \sum_{\mathbf{k}} \sqrt{\frac{2\pi\hbar\omega}{SL(k)}} \frac{a}{d} e^{k_z^{d2} l} \left(\mathbf{e}_{\mathbf{k}} + i \frac{k}{k_z^{d2}} \mathbf{e}_z \right) e^{-k_z^{d2} z} e^{i(\mathbf{k}\mathbf{r} - \omega t)} a_{\mathbf{k}} + H.c., \quad (4)$$

where S is the surface area of the metal-dielectric interface, $L(k)$ is the area of localization of the surface plasmon along the normal to the substrate surface. Here $\mathbf{e}_{\mathbf{k}}$ and \mathbf{e}_z are unit vectors directed respectively along and perpendicular to the surface; $k = |\mathbf{k}|$ is the longitudinal wave number through which the real coefficients are expressed $k_z^m = \sqrt{k^2 - \varepsilon_m(\omega) \cdot \omega^2 / c^2}$, $k_z^{d1(2)} = \sqrt{k^2 - \varepsilon_{d1(2)} \cdot \omega^2 / c^2}$, characterizing the rate of decay of fields at a distance from the metal surface; c is the speed of light, Also in formulas (3)–(5) the notation is introduced: l is the thickness of the intermediate layer; $a = \varepsilon_{d1} k_z^{d2}$, $b = \varepsilon_{d2} k_z^{d1}$, $d = a \text{ch}(k_z^{d1} l) + b \text{sh}(k_z^{d1} l)$ and $f = b \text{ch}(k_z^{d1} l) + a \text{sh}(k_z^{d1} l)$. An expression for the localization region $L(k)$ of the surface plasmon has been obtained, from which it follows that the function $L(k)$ decreases monotonically with an increase in the longitudinal wave number k .

The frequency $\omega(k)$ of the surface plasmon-polariton is the solution of the dispersion equation

$$\frac{\varepsilon_m(\omega)k_z^{d1}}{\varepsilon_{d1}k_z^m} = -\frac{\varepsilon_{d2}k_z^{d1}\text{ch}(k_z^{d1}l) + \varepsilon_{d1}k_z^{d2}\text{sh}(k_z^{d1}l)}{\varepsilon_{d2}k_z^{d1}\text{sh}(k_z^{d1}l) + \varepsilon_{d1}k_z^{d2}\text{ch}(k_z^{d1}l)}. \quad (5)$$

The operator describing the interaction of molecular aggregates with a metal substrate is written as [7]

$$\hat{V} = -\sum_{\mathbf{n}} \hat{\mathbf{p}}_{10} \cdot \hat{\mathbf{E}}(\mathbf{n}),$$

where $\hat{\mathbf{p}}_{10} = N^{-1/2} \sum_{\mathbf{Q}} (\mathbf{p}_{10} B_{\mathbf{Q}}^+ e^{-i\mathbf{Q}\mathbf{n}} + \mathbf{p}_{01}^* B_{\mathbf{Q}} e^{i\mathbf{Q}\mathbf{n}})$ is the operator of the dipole moment of transition in a J-aggregate molecule located at a node with a radius vector \mathbf{n} [8], \mathbf{p}_{10} is the electric dipole moment of the quantum transition of the molecule from the ground to the first excited state; N is the number of molecules in a two-dimensional lattice, $B_{\mathbf{Q}}^+$ and $B_{\mathbf{Q}}$ are the operators of the generation and destruction of excitons with the wave vector \mathbf{Q} .

The matrix element of the EP-interaction operator between the state of a system with one exciton $|1_{ex}, 0_{pl}\rangle$ (without a plasmon), and the state with one plasmon (without an exciton) $|0_{ex}, 1_{pl}\rangle$ has the following form:

$$V_{10,01}(\mathbf{k}) = -\sqrt{\frac{2\pi\hbar\omega}{s \cdot L(k)}} \frac{a}{d} \exp[-k_z^{(d2)}(z-l)] (\mathbf{e}_{\mathbf{k}} \cdot \mathbf{p}_{10}), \quad (6)$$

where s is the area of the unit cell of a two-dimensional monolayer, z is the distance from the metal surface to the monolayer.

In the case of weak EP-coupling, the rate of transition from state $|0_{ex}, 1_{pl}\rangle$ to state $|1_{ex}, 0_{pl}\rangle$ is written as

$$U(\mathbf{k}) = \frac{2\pi}{\hbar} |V_{10,01}(\mathbf{k})|^2 \delta(E_{ex}(\mathbf{k}) - \hbar\omega(k)). \quad (7)$$

As can be seen from (7), the dependence of the transition rate on the wave number has a delta-like peak when the exciton energy and the SPP coincide $E_{ex}(\mathbf{k}) = \hbar\omega(k)$.

If $U^{-1} < \tau_{ex}$, this is effectively the quenching of excitons, i.e. the energy transfer from the Frenkel excitons of the J-aggregate to the metal substrate. According to the calculations performed, the quenching rate is at a maximum of $\sim 10^{13} \text{ s}^{-1}$ with a layer thickness of 15 nm, which is significantly higher than the rates of other processes leading to the death of excitons.

A numerical study of the dependence of the Rabi splitting on the system parameters was carried out for a strong EP-coupling. Figure 2 shows the dispersion laws (1) of hybrid plasmon-exciton states for different values of the dielectric constant of the second medium at fixed values of thickness $l = 10$ nm and the dielectric constant $\varepsilon_{d1} = 2$ of the first medium. The dotted lines correspond to unrelated excitonic and SPP-modes. With increasing permeability ε_{d2} , the intersection point of the exciton and SPP dispersion curves shifts towards large k , and the value of the Rabi splitting decreases from $\Delta G_1 = 84$ meV at $\varepsilon_{d2} = 2$ to $\Delta G_4 = 46$ meV at $\varepsilon_{d2} = 5$.

Thus, the study carried out in [3] showed that the geometric and dielectric characteristics of the considered three-layer structure significantly affect the magnitude of the plasmon-exciton interaction energy. Therefore, depending on the system parameters, the value of Rabi splitting can reach ~ 100 MeV, which is consistent with the experimental data of other authors [8–9]. In addition, varying the permeability and thickness of the interlayer between the metal substrate and the film of J-aggregates, it is possible to change the rate of energy exchange between surface plasmons and Frenkel excitons and achieve unilateral energy transfer to J-aggregates, which is necessary for the development of new organic light emitters.

With a strong exciton-plasmon interaction, it is necessary to describe the energy transformation on the basis of a more general quantum mechanical formalism using a paired density matrix $\hat{\rho}(t)$ of quantum subsystems interacting both with each other and with a thermostat [10–11].

In [11], the kinetics of energy exchange between plasma and exciton subsystems in a planar composite nanostructure with strong exciton-plasmon interaction was investigated. It was shown that the energy trans-

fer between the system components occurs non-monotonically in time, but has the form of damped oscillations depending on the relaxation parameters, the Rabi frequency and the detuning from resonance.

The density operator $\hat{\rho}(t)$ of a multilayer system satisfies a kinetic equation written on the basis of the Neumann equation with a relaxation term — drain

$$\frac{d}{dt}\hat{\rho} = \frac{1}{i\hbar}[\hat{H}_0 + \hat{V}, \hat{\rho}] - \hat{R}^\dagger \hat{\rho}. \quad (8)$$

Operator \hat{H}_0 in eq. (8) is the Hamiltonian of the combined 1+2 system (exciton + plasmon subsystems) in the absence of exciton-plasmon interaction; \hat{R}^\dagger is a relaxation superoperator. In the simplest case of equality of the exciton and plasmon lifetimes $\tau_{pl} = \tau_{exc} = \tau$, an autonomous equation for inversion $\Delta\rho(t) = \rho_{11}(t) - \rho_{22}(t)$ was obtained on the basis of (8) at an arbitrary phase relaxation time T_2 and under conditions of zero detuning from resonance $\Delta E = 0$

$$\Delta\ddot{\rho}(t) + \left(\frac{1}{\tau} + \frac{1}{T_2}\right)\Delta\dot{\rho}(t) + \left(\Omega^2 + \frac{1}{\tau T_2}\right)\Delta\rho(t) = 0, \quad \Omega = 2|V_{12}|/\hbar. \quad (9)$$

Calculations based on equation (9) at equal times $\tau_{pl} = \tau_{exc} \sim 10^{-12}$ c and zero detuning from resonance $\Delta E = 0$ showed that with a decrease in the transverse relaxation time T_2 from $0.8\tau_{exc}$ to $0.05\tau_{exc}$ at the Rabi frequency of $\Omega = 15 \div 20 \cdot 10^{12}$ s⁻¹, a decrease in the depth of population modulation was observed $\rho_{11}(t)$ and $\rho_{22}(t)$ up to its almost complete disappearance. When increased to Ω to $30 \cdot 10^{12}$ s⁻¹, the modulation became clearly pronounced again.

In the general case of arbitrary relations between times $\tau_{pl}, \tau_{exc}, T_2$ and non-zero detuning ΔE from resonance, the kinetics of populations of states 1 and 2 is analyzed on the basis of the modified Johnson-Merrifield equation [12] proposed to describe spin-selective exciton annihilation

$$\frac{d}{dt}\hat{\rho} = -\frac{i}{\hbar}[(\hat{H}_0 + \hat{V}), \hat{\rho}] - \frac{1}{2}\tilde{k}_1\{\hat{P}_1, \hat{\rho}\}_+ - \frac{1}{2}\tilde{k}_2\{\hat{P}_2, \hat{\rho}\}_+ - T_2^{-1}\hat{\rho}, \quad (10)$$

where $\{\hat{P}_j, \hat{\rho}\}_+ = \hat{P}_j \cdot \hat{\rho} + \hat{\rho} \cdot \hat{P}_j$ is the anti-commutator, $\hat{P}_j = |j\rangle\langle j|$ is the projection operator on state j , \tilde{k}_1, \tilde{k}_2 are additives to scalar rates of deactivation of the system through plasmon and exciton decay channels. The solution of the operator equation (10) can be represented using matrix exponentials $\hat{\rho}(t) = \exp(-t/T_2) \cdot \exp(\hat{K}^{(-)}t)\hat{\rho}(0)\exp(\hat{K}^{(+)}t)$, and the kinetic matrix $K_{ij}^{(\mp)}$ is

$$K_{ij}^{(\mp)} = \begin{pmatrix} \mp \frac{i}{\hbar}(\hbar\omega(k) + V_{11}) - \frac{1}{2}\tilde{k}_1 & \mp \frac{i}{\hbar}V_{12} \\ \mp \frac{i}{\hbar}V_{21} & \mp \frac{i}{\hbar}(E_{exc} + V_{22}) - \frac{1}{2}\tilde{k}_2 \end{pmatrix}, \quad (11)$$

with eigenvalues of matrices $K_{ij}^{(\mp)}$ in the form of

$$\kappa_{1,2}^{(\mp)} = (\mp) \frac{i}{2} \left[\omega(k) + E_{exc} / \hbar \right] - \frac{1}{4}(\tilde{k}_1 + \tilde{k}_2) \mp \frac{1}{2} \left\{ \left[i(\mp)\Delta E / \hbar + (\tilde{k}_1 - \tilde{k}_2) / 2 \right]^2 - \Omega^2 \right\}^{1/2}.$$

In particular, the population kinetics of the exciton state $|2\rangle = |1_{ex}, 0_{pl}\rangle$ is determined by the following set of exponents with complex-valued indicators as combinations of the $\kappa_{1,2}^{(\mp)}$ eigenvalues

$$\rho_{22}(t) = \langle 2 | \hat{\rho}(t) | 2 \rangle = \frac{K_{21}^{(-)} K_{12}^{(+)}}{(\kappa_1^{(-)} - \kappa_2^{(-)})(\kappa_1^{(+)} - \kappa_2^{(+)})} \times \\ \times \left[\exp((\kappa_1^{(-)} + \kappa_1^{(+)})t) + \exp((\kappa_2^{(-)} + \kappa_2^{(+)})t) - \exp((\kappa_1^{(-)} + \kappa_2^{(+)})t) - \exp((\kappa_2^{(-)} + \kappa_1^{(+)})t) \right] \quad (12)$$

Based on models (9) and (10)–(12), the parametric dependences of population kinetics $\rho_{11}(t)$ and $\rho_{22}(t)$ an activated planar system with an exciton-bearing J-aggregate layer on a conductive substrate were investigated.

Figures 3 and 4 show the time dependences of the populations of the plasmon and exciton subsystems calculated on the basis of model (10)–(12). At significant differences (up to the order of magnitude and high-

er) in the proper lifetimes of excitons and plasmons τ_{exc}, τ_{pl} , characteristic modulations with the Rabi frequency Ω not only of partial densities $\rho_{11}(t)$ and $\rho_{22}(t)$ quasiparticles, but also of the total excitation density $n(t) = \rho_{11}(t) + \rho_{22}(t)$, with noticeable deviations from the trend exponent, were observed. Increasing the Rabi frequency from $20 \cdot 10^{12}$ to $80 \cdot 10^{12} \text{ s}^{-1}$ resulted in a significant increase in the depth of modulation of the plasmon density $\rho_{11}(t)$ at the ratio of relaxation rates $\tilde{k}_1 = 5.5 \cdot T_2^{-1}$, $\tilde{k}_2 = 0.1 \cdot T_2^{-1}$. At the same time, the modulation of the exciton density $\rho_{22}(t)$ at the Rabi frequency was carried out almost to zero values over time $t \sim \Omega^{-1}$.

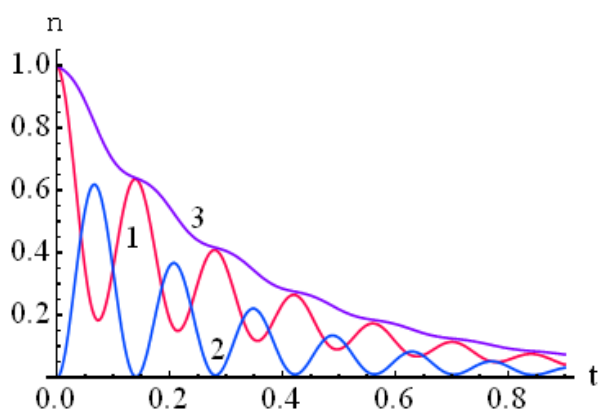


Figure 3. Kinetics of partial populations of plasmon $\rho_{11}(t)$ — (1) and exciton $\rho_{22}(t)$ — (2) subsystems, as well as the total population $n(t) = \rho_{11} + \rho_{22}$ (envelope curve 3) of the excited state of the system, at various additional decay rates $\tilde{k}_1 = 5.5 \cdot T_2^{-1}$, $\tilde{k}_2 = 0.1 \cdot T_2^{-1}$, transverse relaxation time $T_2 = 1 \text{ ps}$ and Rabi frequency $\Omega = 40 \cdot T_2^{-1}$. Time t is expressed in ps. The amount of detuning from the resonance $\Delta E / \hbar = 20 \cdot T_2^{-1}$

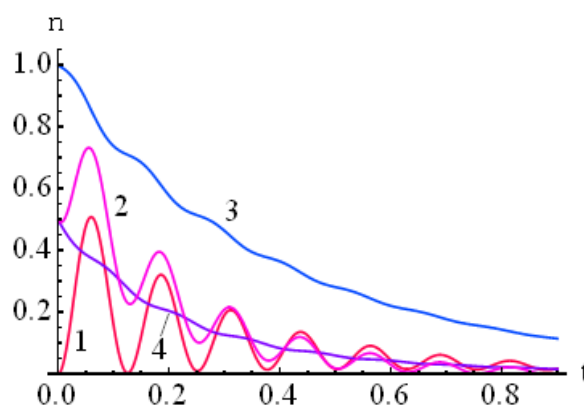


Figure 4. Population kinetics of the exciton $\rho_{22}(t)$ subsystem at the initial settlement of the partial plasmon state $\rho_{11}(0) = 1$ — (1), the pure initial state of the equal-amplitude superposition — (2); the mixed initial state with the same weight coefficients — (4), as well as the total population $n(t) = \rho_{11} + \rho_{22}$ (envelope curve 3) of the excited state of the system. The parameter values are the same as for Figure 3

1.1 Transfer of exciton excitation energy between two monolayers of J-aggregates

In addition to the energy transfer to the plasmon reservoir in the system of Figure 1, the non-radiative transfer of exciton excitation energy between monolayers A and B of molecules of polymethine dyes forming J-aggregates was investigated (Fig. 5). It was assumed that such a distant transfer could be carried out by means of surface plasmons of a nanometer-thick metal film located between the monolayers. The study of multilayered systems containing J-aggregates (JA) of two varieties is important for understanding the processes of energy transfer in biological light-harvesting complexes, as well as for the creation of artificial photosynthesis systems [13].

A number of experimental papers report on the registration of this process. Thus, the authors of [14-15] observed energy transfer between JA layers formed by molecules of various polymethine dyes in a polymer film. As a result of the EP interaction, non-radiative energy transfer $J \rightarrow \text{SPP} \rightarrow J$ occurs with the appearance of the Frenkel exciton in the initially inactive molecular layer. At weak PE-coupling, the energy transfer rate $PP \rightarrow J$ can be calculated on the basis of quantum mechanical perturbation theory [16].

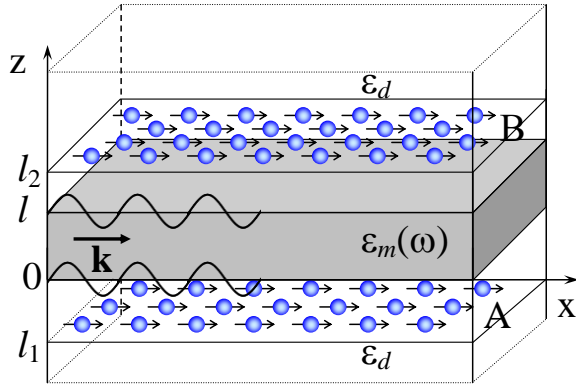


Figure 5. Location of the metal film between two monolayers of J-aggregates

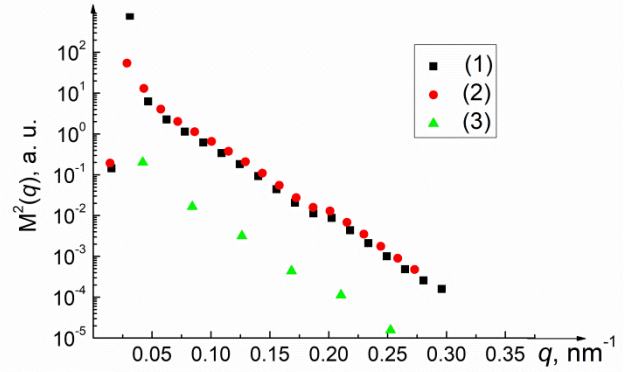


Figure 6. Dependence of the square of a composite matrix element on the wave number for different wave vectors: 1 — $\mathbf{q} \parallel \mathbf{q}_a$, 2 — $\mathbf{q} \parallel \mathbf{q}_a + \mathbf{q}_b$, 3 — $\mathbf{q} \parallel \mathbf{q}_a - \mathbf{q}_b$

The exciton excitation energy transfer rate from one monolayer to another using surface plasmons of the metal film can be determined in the second order of quantum mechanical perturbation theory

$$U_{AB} = \frac{2\pi}{\hbar} \sum_{\mathbf{q}, \mathbf{q}'} P_{\mathbf{q}} |M(\mathbf{q}, \mathbf{q}')|^2 \delta(E_A(\mathbf{q}) - E_B(\mathbf{q}')), \quad (13)$$

where $M(\mathbf{q}, \mathbf{q}')$ is a composite matrix element of EP-interaction defined by the expression

$$M(\mathbf{q}, \mathbf{q}') = \sum_{\mathbf{k}, j} \left[\frac{\langle \mathbf{q}' | \hat{V}_{pl-exB}^{(j)} | \mathbf{k} \rangle \langle \mathbf{k} | \hat{V}_{pl-exA}^{(j)} | \mathbf{q} \rangle}{E_A(\mathbf{q}) - \hbar\omega_k^{(j)}} \right]. \quad (14)$$

The following designations are introduced in formulas (13) and (14): the initial state of the system $|\mathbf{q}\rangle = |1_{ex}^A, 0_{ex}^B, 0_{pl}\rangle$ is the exciton state of monolayer A, the final state $|\mathbf{q}'\rangle = |0_{ex}^A, 1_{ex}^B, 0_{pl}\rangle$ is the exciton state of monolayer B, $|\mathbf{k}\rangle = |0_{ex}^A, 0_{ex}^B, 1_{pl}\rangle$ is an intermediate plasmon state characterized by a wave vector \mathbf{k} . Summation by j takes into account the possibility of excitation in a thin film of two types of surface plasmons: anti-symmetric (high-frequency $\omega_k^{(1)}$) and symmetric ($\omega_k^{(2)}$ low-frequency), $E_A(\mathbf{q})$ and $E_B(\mathbf{q}')$ are exciton excitation energies in monolayers A and B, $P_{\mathbf{q}}$ is the population of exciton states described by the Boltzmann distribution.

To calculate the matrix elements of the plasmon-exciton interaction operator $\hat{V}_{pl-ex}^{(j)} = -\sum_{\mathbf{n}} \mathbf{d}(\mathbf{n}) \cdot \mathbf{E}^{(j)}(\mathbf{n})$ included in (14), it is convenient to use the secondary quantization formalism. The operator $\mathbf{d}(\mathbf{n})$ of the dipole moment of transition JA to the exciton state is written in this formalism as

$$\mathbf{d}(\mathbf{n}) = \frac{1}{\sqrt{N}} \sum_{\mathbf{q}} (\mathbf{d}_{01} e^{i\mathbf{q}\mathbf{n}} B_{\mathbf{q}} + \mathbf{d}_{10} e^{-i\mathbf{q}\mathbf{n}} B_{\mathbf{q}}^+), \quad (15)$$

where \mathbf{d}_{10} is the dipole moment of transition in a J-aggregate molecule between its ground and first excited states, \mathbf{n} is the vector specifying the position of the molecule in JA, N is the number of molecules in JA, $B_{\mathbf{q}}$ and $B_{\mathbf{q}}^+$ are the exciton destruction and generation operators. The electric field strength operators of the surface plasmon mode j can be found in the same way as in [3]. In a dielectric medium at $z < 0$ (Fig. 5), the intensity decreases exponentially with distance from the metal film

$$\mathbf{E}_d^{(j)}(\mathbf{n}, z, t) = \sum_{\mathbf{k}} \sqrt{\frac{2\pi\hbar\omega_k^{(j)}}{S L^{(j)}(k)}} \left(1 \mp e^{-k_m^{(j)} l} \right) e^{k_d^{(j)} z} \left(\mathbf{e}_{\mathbf{k}} - i \frac{k}{k_d^{(j)}} \mathbf{e}_z \right) e^{i(\mathbf{k}\mathbf{n} - \omega_k^{(j)} t)} a_{\mathbf{k}} + H.c. \quad (16)$$

In the area of metal $0 \leq z \leq l$, the tension has the complicated form

$$\mathbf{E}_m^{(j)}(\mathbf{n}, z, t) = \sum_{\mathbf{k}} \sqrt{\frac{2\pi\hbar\omega_k^{(j)}}{S L^{(j)}(k)}} \left[\left(\mathbf{e}_{\mathbf{k}} + i \frac{k}{k_m^{(j)}} \mathbf{e}_z \right) e^{-k_m^{(j)} z} \mp \left(\mathbf{e}_{\mathbf{k}} - i \frac{k}{k_m^{(j)}} \mathbf{e}_z \right) e^{k_m^{(j)}(z-l)} \right] e^{i(\mathbf{k}\mathbf{n} - \omega_k^{(j)} t)} a_{\mathbf{k}} + H.c. \quad (17)$$

At the same time $z > l$, an exponential decrease of field strength with distance is observed

$$\mathbf{E}_d^{(j)}(\mathbf{n}, z, t) = \mp \sum_{\mathbf{k}} \sqrt{\frac{2\pi\hbar\omega_k^{(j)}}{S L^{(j)}(k)}} \left(1 \mp e^{-k_{mz}l}\right) e^{-k_{dz}^{(j)}(z-l)} \left(\mathbf{e}_{\mathbf{k}} + i \frac{k}{k_{dz}^{(j)}} \mathbf{e}_z\right) e^{i(\mathbf{k}\mathbf{n} - \omega_k^{(j)}t)} a_{\mathbf{k}} + H.c., \quad (18)$$

where the "-" sign refers to the antisymmetric, the "+" sign refers to the symmetric plasmon. In formulas (16)–(18), the surface area of the film is indicated by S ; $a_{\mathbf{k}}$ is the plasmon destruction operator. The frequency $\omega_k^{(j)}$ of the surface plasmon is the solution of the following dispersion equation [16]

$$e^{k_{mz}l} = \mp \frac{\varepsilon_m(\omega)k_{dz} - \varepsilon_d k_{mz}}{\varepsilon_m(\omega)k_{dz} + \varepsilon_d k_{mz}}, \quad (19)$$

where are the coefficients $k_{dz} = \sqrt{k^2 - \varepsilon_d \omega^2/c^2}$, and $k_{mz} = \sqrt{k^2 - \varepsilon_m(\omega) \omega^2/c^2}$ as in the single-layer case, the rate of decrease in the field strength of the surface plasmon is determined as it moves away from the metal-dielectric interface; $\varepsilon_m(\omega) = \varepsilon_{\infty} - \omega_{pl}^2/\omega^2$ is the dielectric constant of the metal in the generalized Drude model, ε_d is the frequency-independent dielectric constant of the medium surrounding the metal film, ε_{∞} is the high-frequency dielectric constant of the metal, ω_{pl} is the plasma frequency of the metal.

The function $L^{(j)}(k)$, as in the single-layer case, has a length dimension and characterizes the width of the localization region of the surface plasmon in the direction normal to the surface of the metal film [16]. In the quasi-static approximation, when $c \rightarrow \infty$, $k_{mz}, k_{dz} \rightarrow k$, the coefficient $L^{(j)}(k)$ is greatly simplified

$$L^{(j)}(k) = \frac{2}{k} \frac{\omega_{pl}^2}{\omega_k^{(j)2}} (1 - e^{-2kl})$$

and the frequencies of antisymmetric and symmetric plasmons can be written explicitly

$$\omega_k^{(1)2} = \frac{\omega_p^2(1 + e^{kl})}{\varepsilon_{\infty}(1 + e^{kl}) - \varepsilon_d(1 - e^{kl})}, \quad \omega_k^{(2)2} = \frac{\omega_p^2(1 - e^{kl})}{\varepsilon_{\infty}(1 - e^{kl}) - \varepsilon_d(1 + e^{kl})}. \quad (20)$$

Formulas (16)–(18) for the electric field strengths of the surface plasmon pass into the expressions obtained and used in [4].

Matrix elements of the EP interaction operator $\hat{V}_{pl-ex}^{(j)}$ have the following form:

$$\langle \mathbf{k} | \hat{V}_{pl-ex}^{(j)} | \mathbf{q} \rangle = \sqrt{\frac{2\pi\hbar\omega_k^{(j)}}{s_A L^{(j)}(k)}} (\mathbf{d}_{10}^A \cdot \mathbf{e}_{\mathbf{k}}) \left(1 \mp e^{-k_{mz}l}\right) e^{-k_{dz}^{(j)}l_1} \delta_{\mathbf{k}, \mathbf{q}}, \quad (21)$$

$$\langle \mathbf{q}' | \hat{V}_{pl-ex}^{(j)} | \mathbf{k} \rangle = \mp \sqrt{\frac{2\pi\hbar\omega_k^{(j)}}{s_B L^{(j)}(k)}} (\mathbf{d}_{01}^B \cdot \mathbf{e}_{\mathbf{k}}) \left(1 \mp e^{-k_{mz}l}\right) e^{-k_{dz}^{(j)}(l_2-l)} \delta_{\mathbf{k}, \mathbf{q}'}, \quad (22)$$

where $s_{A(B)}$ is the unit cell area of monolayer A(B), $l_1(l_2)$ is the distance from the lower surface of the film to monolayer A(B). The Kronecker symbol $\hat{V}_{pl-ex}^{(j)}$ in the operator expresses the equality of the exciton wave vectors and the intermediate surface plasmon, which, in turn, leads to the equality of the exciton wave vectors \mathbf{q} and \mathbf{q}' in monolayers A and B.

Substitution (21), (22) in (14) gives the following expression for a composite matrix element:

$$M(\mathbf{q}, \mathbf{q}) = \frac{2\pi}{\sqrt{s_A s_B}} d_{01}^A d_{10}^B \cos \alpha \cos \beta \sum_j (\mp) \frac{\hbar\omega_q^{(j)}}{L^{(j)}(q)} \frac{\left(1 \mp e^{-k_{mz}^{(j)}l}\right)^2 e^{-k_{dz}^{(j)}(l_1+l_2-l)}}{E_A(\mathbf{q}) - \hbar\omega_q^{(j)}}, \quad (23)$$

where α and β are the angles between the exciton wave vector and the dipole transition moments in the molecules of J-aggregates A and B.

It should be noted that the rate of direct transfer of exciton excitation energy from monolayer A to monolayer B due to the dipole-dipole interaction between monolayer molecules can also be found by formula (13), in which the matrix element $M_1(\mathbf{q}, \mathbf{q}')$ of the dipole-dipole interaction energy operator is used instead of a composite matrix element, taking into account delocalization molecular excitation

$$M_1(\mathbf{q}, \mathbf{q}') = \sum_{\mathbf{n}, \mathbf{m}} \left[\frac{\mathbf{d}_{01}^A \mathbf{d}_{10}^B}{\epsilon_d r_{\mathbf{nm}}^3} - 3 \frac{(\mathbf{r}_{\mathbf{nm}} \mathbf{d}_{01}^A)(\mathbf{r}_{\mathbf{nm}} \mathbf{d}_{10}^B)}{\epsilon_d r_{\mathbf{nm}}^5} \right] e^{i\mathbf{q}\mathbf{n}} e^{-i\mathbf{q}'\mathbf{m}},$$

where $r_{\mathbf{nm}}$ is the distance between molecules position of which is given by the vector \mathbf{n} in one monolayer and the vector \mathbf{m} in the other. If we consider the number of molecules forming each monolayer $N \rightarrow \infty$, then the matrix element $M_1(\mathbf{q}, \mathbf{q}')$ will be diagonal. Also in this case, a continuum approximation can be used, in which summation is replaced by integration. Then, provided that $\mathbf{d}_{01}^A = \mathbf{d}_{10}^B = \mathbf{d}_{10}$, the following expression for a matrix element is obtained [16].

$$M_1(\mathbf{q}, \mathbf{q}) = \frac{2\pi}{\epsilon_d \sqrt{S_A S_B}} d_{10}^2 q e^{-q l_{AB}} \cos^2 \alpha, \quad (24)$$

where l_{AB} is the distance between monolayers.

To make the energy transfer efficient, monolayers of J-aggregates with the closest possible positions of absorption and luminescence spectra were selected as energy donors and acceptors. In particular, J-aggregates of pseudoisocyanine (PIC) and the dye 5,5',6,6'-tetrachloro-1,1'-diethyl-3,3'-bis(4-sulfopropyl)-benzimidazolocarbo-cyanine (TDBC), absorption spectra maxima of which are located at ~ 590 nm (2.1 eV), satisfy this condition [16]. In another variant, the same JA can be considered as an energy donor and acceptor. During the calculations, it was assumed that both the donor and the acceptor were J-aggregates of the TDBC dye, and in both monolayers there were $N = 500$ molecules in each direction of the elementary vectors. The dipole moment of the transition in the TDBC molecule is co-directional with the elementary vector \mathbf{a} and is equal to $|d_{10}| \approx 10$ D. The width of the Lorentz contour at half the height was assumed to be equal to $\Gamma = 0.05$ eV. In all calculations, the temperature was considered equal to $T = 300$ K. Silver was chosen as the material of the conductive film, for which the plasma frequency is $\hbar\omega_{pl} = 9.1$ eV and the high-frequency dielectric permittivity is $\epsilon_\infty = 3.7$. The dielectric constant of the medium surrounding the film was $\epsilon_d = 2$.

Figure 6 shows the results of calculations of the square of a composite matrix element according to formula (23) for different values and directions of the wave vector \mathbf{q} . Calculations were carried out for a film with a thickness of $l = 10$ nm and the distances from the donor monolayer A and the acceptor monolayer B to the lower surface of the film $l_1 = 5$ nm and $l_2 = 20$ nm, respectively. It should be noted that the distance l_1 remained unchanged in all calculations. As can be seen from the figure, the matrix element reaches the highest values in the region of small quantum numbers $q \sim 10^5$ cm $^{-1}$, since the energy difference between exciton and plasmon is minimal in this region. In addition, the values of the matrix element are small (points 3) if the exciton propagates almost perpendicular to the direction of the dipole moment of transition, which follows from formula (23).

Table

Dependence of the energy transfer rate on the distance between monolayers

Distance between surfactant monolayers l_{AB} , nm	The rate of energy transfer through the film U_{AB} , s $^{-1}$	The rate of energy transfer in the dielectric U'_{AB} , s $^{-1}$
15	$3.85 \cdot 10^{12}$	$3.98 \cdot 10^9$
20	$2.19 \cdot 10^{12}$	$1.70 \cdot 10^9$
25	$1.24 \cdot 10^{12}$	$8.32 \cdot 10^8$
30	$7.07 \cdot 10^{11}$	$4.52 \cdot 10^8$

The dependences of the rate of non-radiative energy transfer on the distance h between the monolayer B and the film surface at different film thicknesses were determined. Calculations showed that energy transfer occurs mainly due to symmetric plasmons. The field strength of plasmons of this type decreases with increasing film thickness.

Table presents data illustrating the effect of a 5 nm thick conductive film on the energy transfer rate between JA monolayers. The distance from monolayer B to the surface of the film varied. The table shows that in the presence of a metal film, energy transfer is more efficient than directly in a dielectric at the same distance.

Thus, in [16] there was constructed and numerically implemented a mathematical model of the energy transfer of a two-dimensional Frenkel exciton from one JA monolayer to another by means of surface plas-

mons of a metal film placed between the monolayers. It was shown that the presence of a conductive film significantly increases the rate of non-radiative energy transfer. In addition, the distance over which the energy can be efficiently transmitted increases several times compared to transmission in a dielectric. This circumstance may be useful in the development of modern optoelectronic devices based on new physical principles of operation.

1.2 Energy transfer in a cylindrical nanostructure consisting of a metal core and a coaxial shell with phosphor molecules

Light absorption and non-radiative exchange of electron excitation energy between a circular metal nanowire and phosphor molecules surrounding it were investigated on the basis of the above concepts [17]. In the case of molecules not interacting with each other, calculations of the energy transfer rate from a single excited molecule to a nanowire and the decay kinetics of the excited state of the phosphor were carried out. For molecules combined in J-aggregate complexes, the energy transfer rate from a coaxial monolayer formed by J-aggregates to a nanowire was calculated and the possibility of a hybrid exciton-plasmon state was shown. A significant influence of the geometric characteristics of the considered systems on the rate of transformation of the energy of electronic excitation was revealed.

For the rate of energy transfer from the excited phosphor molecule to the nanowire, it is possible to obtain

$$\bar{U}(r) = \frac{4|\mathbf{p}_{01}|^2}{3\hbar} \int_0^\infty \left\{ \frac{\omega_0(k)}{S_0(k)} \frac{I_0^2(q_m R)}{K_0^2(q_d R)} \left[\frac{k^2}{q_d^2} K_0'^2(q_d r) + K_0^2(q_d r) \right] G(\omega_0(k)) + 2 \sum_{n=1}^\infty \frac{\omega_n(k)}{S_n(k)} \frac{I_n^2(q_m R)}{K_n^2(q_d R)} G(\omega_n(k)) \right. \\ \left. \times \left[\left(\frac{k}{q_d} K_n'(q_d r) + \frac{\omega_n(k) n f}{q_d^2 r} K_n(q_d r) \right)^2 + \left(\frac{n k}{q_d^2 r} K_n(q_d r) + \frac{\omega_n(k) f}{q_d} K_n'(q_d r) \right)^2 + K_n^2(q_d r) \right] \right\} dk, \quad (25)$$

where \mathbf{p}_{01} is the matrix element of the electric dipole moment of the quantum transition of the molecule from the first excited state to the ground state, r is the distance between the molecule and the axis of the nanowire, $G(\omega)$ is the emission spectrum of the phosphor molecule. In formula (25), the averaging is performed along the directions of the dipole moment of the transition of the molecule. In the case when the nanowire is surrounded by a monolayer of organic molecules in the J-aggregate state, an energy exchange between the Frenkel excitons of the monolayer and the surface plasmons of the nanowire is possible. The matrix element $V_{10,01}$ of the operator $\hat{V} = -\sum_{\mathbf{n}} \hat{\mathbf{p}}_{01} \cdot \hat{\mathbf{E}}(\mathbf{n})$ of interaction of J-aggregate molecules with the electric field of a

surface plasmon between the states $|1_{ex}, 0_{pl}\rangle$ of the system under consideration (with one exciton and without plasmons) and $|0_{ex}, 1_{pl}\rangle$ (with one plasmon and without excitons) takes the form

$$V_{10,01}^{(n)} = -\sqrt{\frac{4\pi\hbar r \omega_n(k)}{s S_n(k)}} \frac{I_n(q_m R)}{K_n(q_d R)} \times \left[\left(\frac{n k_z}{q_d^2 r} K_n(q_d r) + \frac{\omega_n(k) f}{q_d} K_n'(q_d r) \right) (\mathbf{p}_{01})_\phi + K_n(q_d r) (\mathbf{p}_{01})_z \right] \delta_{k_z, q_1} \delta_{n, q_2 r}, \quad (26)$$

where s is the area of the unit cell of the monolayer. As can be seen from the obtained formula, axisymmetric ($n = 0$) surface plasmons interact only with excitons propagating along the axis of the nanowire ($q_2 = 0$). In other cases, the exciton wave vector has a component along the circumference of the cylinder. $I_n(q_m R), K_n(q_d R)$ are Bessel functions of an imaginary argument.

In the case of strong plasmon-exciton coupling, the conditions for the applicability of the perturbation theory are not fulfilled, and it is necessary to use the density matrix formalism to describe the kinetics of energy exchange as in papers [10-11].

2. Magnetic field modulation of the rate of triplet-triplet annihilation of electronic excitations in nanostructures

The course of spin-selective reactions involving the annihilation of triplet (T) excitons or T-electron excitations localized on molecules is carried out in different ways, depending on how the migration of reagents occurs in a coherent T-T pair [18–20]. In nanostructured systems, the mobility of molecules involved in the reaction depends significantly on the structural features of such systems, and the mechanism of spatial movement of reagent particles reflects either the dynamics of conformational rearrangements of structural

subunits (in the case of “soft-systems”) [18], or the shape of the potential field [19] formed by the system, or both together.

In nanostructures with bistable spatial states, depending on which spatial configuration the T-T pair is in (in a “dense” or “loose” state), we introduce the corresponding density operators $\rho_1(t)$ and $\rho_2(t)$. Thus, the subscript will indicate that the mobile T-molecule belongs to a potential well 1 or 2. The frequencies of jumps Γ_1 and Γ_2 between the pits will be assumed to be different and constant. Then we can write the following system of equations [19]:

$$\begin{cases} \frac{d}{dt}\rho_1(t) = -\frac{i}{\hbar}[H, \rho_1(t)] - \frac{1}{2}\{\rho_1\Lambda + \Lambda\rho_1\} - K_{-1}\rho_1(t) - \Gamma_1\rho_1(t) + \Gamma_2\rho_2(t) \\ \frac{d}{dt}\rho_2(t) = -\frac{i}{\hbar}[H_0, \rho_2(t)] - K_{-2}\rho_2(t) + \Gamma_1\rho_1(t) - \Gamma_2\rho_2(t) \end{cases}, \quad (27)$$

where the spin-Hamiltonian H_0 of a “loose” T-T-pair does not contain an exchange interaction. The annihilation operator Λ in (27) is determined through the projector on the singlet state of the T-T-pair: $\Lambda = K_S|00\rangle\langle 00|$ and a fixed rate $U(r_{ann}) = K_S$. For the density operator $\rho_1(t)$ we obtain ($U(t) = \exp(Kt)$, $K = -iH/\hbar - \Lambda/2$)

$$\rho_1(t) = \exp(-\alpha_1 t)U(t) \left[\rho_1(0) + \Gamma_2 \left(\int_0^t \exp(-\alpha_1 t')U(-t')\rho_2(t')U^*(-t')dt' \right) \right] U^*(t). \quad (28)$$

We can write a similar equation for the density operator $\rho_2(t)$

$$\rho_2(t) = \exp(-\alpha_2 t)U_0(t) \left[\rho_2(0) + \Gamma_1 \left(\int_0^t \exp(-\alpha_2 t')U_0^+(t')\rho_1(t')U_0(t')dt' \right) \right] U_0^+(t). \quad (29)$$

The unitary operators $U_0(t) = \exp(-iH_0 t/\hbar)$ and $U_0^+(t) = \exp(iH_0 t/\hbar)$ introduced in (29) are related to the Hamiltonian H_0 determining the evolution of the T-T pair in its “loose” configuration (coherent T excitations are spaced in different pits 1 and 2).

Substituting (29) into (28) we obtain an exact integral equation for the density operator $\rho_1(t)$ ($\Delta\alpha = \alpha_1 - \alpha_2$)

$$\begin{aligned} U(-t)\rho_1(t)U^*(-t) = \exp(-\alpha_1 t) \left[\rho_1(0) + \Gamma_2 \left(\int_0^t \exp(\Delta\alpha t')U(-t')U_0(t')\rho_2(0)U_0^+(t')U^*(-t')dt' \right) + \right. \\ \left. + \Gamma_1\Gamma_2 \left(\int_0^t \exp(\Delta\alpha t')U(-t')U_0(t') \left(\int_0^{t'} \exp(\alpha_2 t'')U_0^+(t'')\rho_1(t'')U_0(t'')dt'' \right) U_0^+(t')U^*(-t')dt' \right) \right] \end{aligned} \quad (30)$$

To construct approximations of solutions of the basic integral equation (30), an iterative procedure can be organized following one of two paths:

1) For the integral term, the first term $\rho_1^{(0)}(t)$ of the right part (30) can be used as the zero approximation operator

$$\rho_1^{(0)}(t) = \exp(-\alpha_1 t)U(t)\rho_1(0)U^*(t). \quad (31)$$

2) The sum of the first two terms of the right part (30) can be used as the zero approximation operator $\rho_1^{(0)}(t)$.

In another typical variant of the initial condition $\rho_2(0) = 0$, in the approximation of one-time returns to pit 1, we obtain a closed solution. The matrix element $\rho_{SS}(t) = \langle 00|\rho_1(t)|00\rangle$ determining the population dynamics of a paired singlet state can be calculated based on Sylvester’s theorem for matrix exponentials.

It can be seen from the matrix $\langle J|K|J'\rangle$ structure that the mixing of spin states $|00\rangle$ and $|10\rangle$ is a consequence of the difference in the g-factors of excitations and, in addition, the relationship between spin states $|00\rangle$ and $|20\rangle$ appears as a result of intramolecular spin-spin interaction.

In [20] the effect of a magnetic field generated by a ferromagnetic nanoparticle on the annihilation of triplet-excited organic molecules or triplet excitons in a near-surface particle layer was studied. A detailed mathematical model has been presented that accounts for electron excitation diffusive mobility and geometry of the system.

We define the coordinate-spin density operator $\hat{\rho}(\mathbf{r}_1, \mathbf{r}_2, t | \mathbf{r}'_1, \mathbf{r}'_2, \mathbf{B}(\mathbf{r}_1), \mathbf{B}(\mathbf{r}_2))$ determining the population growth rate of the state $|JM\rangle$ optimal for the reaction (here J, M are the total spin moment and its z-projection correspondingly). For the rate constant $K(\mathbf{r}'_1, \mathbf{r}'_2)$ of the spin-selective triplet (T) states annihilation the following holds

$$K(\mathbf{r}'_1, \mathbf{r}'_2) = \int_0^\infty dt \iint_{\Delta V_R} U(|\mathbf{r}_1 - \mathbf{r}_2|) \frac{1}{2} \text{Tr} \{ P_S, \hat{\rho}(\mathbf{r}_1, \mathbf{r}_2, t | \mathbf{r}'_1, \mathbf{r}'_2, \mathbf{B}(\mathbf{r}_1), \mathbf{B}(\mathbf{r}_2)) \}_+ d^3 r_1 d^3 r_2, \quad (32)$$

where $\text{Tr} \{ P_S, \hat{\rho} \}_+ = \sum_{J,M} \langle JM | (P_S \hat{\rho} + \hat{\rho} P_S) | JM \rangle = \langle 00 | \hat{\rho} | 00 \rangle$, because $P_S = |00\rangle\langle 00|$ is the operator performing a projection of the T-T pair singlet state; $\mathbf{r}'_1, \mathbf{r}'_2$ are the initial positions of the mobile particles. ΔV_R is integration volume (volume of the layer between the ferromagnetic particle and the inner surface of the nanoreactor); $U(r)$ is the distance-dependent rate of an annihilation act. The kinetic operator is given in the complete 9x9 basis of triplet-triplet pair spin states. Time dependencies of the singlet spin state population of the triplet-triplet pair and the dependence of the triplet-triplet annihilation magnetic response profile (magnetic reaction effect) from the magnetic field induction were obtained. It was found that the influence of a magnetic field gradient on the reaction yield dominates over the other known mechanisms of spin-dynamics in triplet-triplet pairs.

Conclusions

A series of works by the authors [3–5, 10, 11 and 16-20] laid the foundations for a general quantum description of the features of exciton-plasmon and exciton-exciton interaction in hybrid organometallic nanosystems, as well as the kinetics of photo-transformations of quasiparticles, taking into account the mesoscopic specificity inherent in such nanosystems.

Acknowledgments

The research was carried out with the financial support of the Ministry of Science and Higher Education of the Russian Federation within the framework of the scientific project No. FSGU-2023-0003.

References

- 1 Zayats, A.V. & Richards, D. (2009). *Nanooptics and near-field optical microscopy*. Boston, Boston: Artech House.
- 2 Gonzalez-Tudela, A., Huidobro, P.A., Martín-Moreno, L., Tejedor, C. & Garcia-Vidal, F.J. (2013). Theory of Strong Coupling between Quantum Emitters and Propagating Surface Plasmons. *Phys. Rev. Lett.*, *110*, 126801. <https://doi.org/10.1103/PhysRevLett.110.126801>
- 3 Chmereva, T.M., Kucherenko, M.G. & Kurmangaleev, K.S. (2016). The plasmon-exciton interaction in layered nanostructures with two-dimensional J-aggregates. *Optics and Spectroscopy*, *120*(6), 881–887. <https://doi.org/10.1134/S0030400X16060060>
- 4 Chmereva, T.M. & Kucherenko, M.G. (2015). Intermolecular radiationless electronic excitation energy transfer near a conductive film. *Russian Physics Journal.*, *57*(10), 1428–1435. <https://doi.org/10.1007/s11182-015-0399-7>
- 5 Chmereva, T.M., Kucherenko, M.G. & Dmitriev, A.D. (2015). Quenching of excited electronic states of quantum dots by a metallic nanowire. *Optics and Spectroscopy*, *118*(2), 284–289. <https://doi.org/10.1134/S0030400X15020058>
- 6 Archambault, A., Marquier, F., Greffet, J.-J. & Arnold, C. (2010). Quantum theory of spontaneous and stimulated emission of surface plasmons. *Phys. Rev B*, *82*, 035411. <https://doi.org/10.1103/PhysRevB.82.035411>
- 7 Goliney, I.Yu., Sugakov, V.I., Valkunas, L. & Vertsimkha, G.V. (2012). Effect of metal nanoparticles on energy spectra and optical properties of peripheral light-harvesting LH2 complexes from photosynthetic bacteria. *Chem. Phys.*, *404*, 116–122. <http://dx.doi.org/10.1016/j.chemphys.2012.03.011>
- 8 Balci, S., Kocabas, C., Ates, S., Karademir, E., Salihoglu, O. & Aydinli, A. (2012). Tuning surface plasmon-exciton coupling via thickness dependent plasmon damping. *Phys. Rev B*, *86*, 235402. <https://doi.org/10.1103/PhysRevB.86.235402>
- 9 Bellessa, J., Symonds, C., Laverdant, J., Benoit, J. -M., Plenat, J.C. & Vignoli, S. (2014). Strong Coupling between Plasmons and Organic Semiconductors. *Electronics*, *3*, 303-313. <https://doi.org/10.3390/electronics3020303>

- 10 Kucherenko, M.G. & Chmereva, T.M. (Eds.). (2016). Proceedings from BPO 2016: *IX International Conference «Basic Problems of Optics-2016»*. St. Petersburg: ITMO University.
- 11 Kucherenko, M.G. & Chmereva, T.M. (2018). Energy exchange dynamics and relaxation of excitations upon strong exciton–plasmon interaction in a planar nanostructure of molecular J-aggregates on a metal substrate. *Optics and Spectroscopy*, 125(2), 173–183. <https://doi.org/10.1134/S0030400X18080179>
- 12 Johnson, R.C. & Merrifield, R.E. (1970). Effects of Magnetic Fields on the Mutual Annihilation of Triplet Excitons in Anthracene Crystals. *Phys. Rev. B.*, 1(2), 896–902. <https://doi.org/10.1103/PhysRevB.1.896>
- 13 Coles, D.M., Somaschi, N., Michetti, P. et.al. (2014). Polariton-mediated energy transfer between organic dyes in a strongly coupled optical microcavity. *Nature Materials*, 13, 712–719. <https://doi.org/10.1038/nmat3950>
- 14 Nakajima, H., Kometani, N., Asami, K. & Yonezawa, Y. (2001). Excitation energy transfer between J-aggregates in layer-by-layer alternate assemblies. *J. Photochem. Photobiol. A: Chemistry*, 143, 161–167. [https://doi.org/10.1016/S1010-6030\(01\)00491-9](https://doi.org/10.1016/S1010-6030(01)00491-9)
- 15 Petrenko, V.Yu., Dmitriev, O.P., Slominskii, Yu.L. & Smirnova, A.L. (2015). Efficient energy transfer between J-aggregates of thiamonomethinecyanine dyes. *Chem. Phys. Lett.*, 621, 22–28. <https://doi.org/10.1016/j.cplett.2014.12.054>
- 16 Chmereva, T.M. & Kucherenko, M.G. (2018). Radiationless Electronic Excitation Energy Transfer Between Monolayers of J-aggregates. *Russian Physics Journal*, 61, 304–311. <https://doi.org/10.1007/s11182-018-1402-x>
- 17 Kucherenko, M.G. & Chmereva, T.M. (2017). Energy Transfer in a Cylindrical Nanostructure Consisting of a Metal Wire and a Coaxial Covering with Luminophore Molecules. *Journal of Applied Spectroscopy*, 84, 382–390. <https://doi.org/10.1007/s10812-017-0480-9>
- 18 Kucherenko, M.G. & Dusembaev, R.N. (2010). Positive magnetic field effect on mutual triplet triplet annihilation of mixed molecular pairs: Magnetosensitive geterofusion induced by difference of g-factors. *Chem. Phys. Lett.*, 487, 58–61. <https://doi.org/10.1016/j.cplett.2010.01.016>
- 19 Kucherenko, M.G. & Pen'kov, S.A. (2014) External magnetic field effect on the rate of mutual annihilation of triplet electronic excitations in nanostructures with bistable spatial states. *Chemical Physics and Mesoscopy*, 16(4), 574–587. <https://www.elibrary.ru/contents.asp?id=34040736>
- 20 Kucherenko, M.G. & Neyasov, P.P. (2022). Spin-selective interaction of triplet-excited molecules on the surface of a ferromagnetic nanoparticle. *Eurasian Physical Technical Journal*, 19(4), 5–16. <https://doi.org/10.31489/2022No4/5-16>

Information about authors*

Kucherenko, Michael Gennad'evich (*corresponding author*) — Doctor of Physical and Mathematical Sciences, Professor, Leading researcher, Professor, Orenburg State University, 460018, Orenburg, Russia; e-mail: clibph@yandex.ru; <https://orcid.org/0000-0001-8821-2427>

Chmereva, Tatiana Mihajlovna — Doctor of Physical and Mathematical Sciences, Associate Professor, Senior researcher, Professor, Orenburg State University, 460018, Orenburg, Russia; e-mail: chmereva@yandex.ru; <https://orcid.org/0000-0003-3111-7853>

*The author's name is presented in the order: *Last Name, First and Middle Names*